Bioorganic & Medicinal Chemistry Letters 19 (2009) 3128–3135

Contents lists available at ScienceDirect

Bioorganic & Medicinal Chemistry Letters

journal homepage: www.elsevier.com/locate/bmcl

Chloro-oxime derivatives as novel small molecule chaperone amplifiers

Yuefen Zhou *, Khang Vu, Yongsheng Chen, John Pham, Thomas Brady, Gang Liu, Jinhua Chen, Joonwoo Nam, P. S. Murali Mohan Reddy, Qingyan Au, Il Sang Yoon, Marie-Helene Tremblay, Gary Yip, Charmian Cher, Bin Zhang, Jack R. Barber, Shi Chung Ng

CytRx Corporation, 3030 Bunker Hill Street, Suite 101, San Diego, CA 92109, USA

ARTICLE INFO

Article history:
Received 10 February 2009
Revised 2 March 2009
Accepted 4 March 2009
Available online 9 March 2009

Keywords:
Small molecule chaperone amplifiers
Protein misfolding
HSF1, heat shock proteins (HSPs)
Stress granule
MG-132 stress
PolyQ stress
ER stress
Neurodegenerative diseases
Cytoprotection
Chloro-oxime derivatives

ABSTRACT

Chloro-oxime derivatives were investigated as novel small molecule chaperone amplifiers. Lead optimization led to the discovery of compounds that displayed potent HSF1 activation activity, significant cytoprotection in MG-132 stress, ER stress and PolyQ stress cell models (EC_{50} < 10 μM).

Neurodegenerative disease is a condition in which cells of the brain and spinal cord become dysfunctional and ultimately die, leading to disabilities in memory, movement, sensory processing and decision making. At present there are few effective pharmaceuticals for the wide range of neurodegenerative diseases and none of them can provide a cure. Therefore there are significant unmet medical needs to find better therapies and approaches to treat neurodegenerative diseases.

In recent years, substantial experimental evidence has accumulated indicating that protein misfolding may be a universal underlying mechanism in the pathogenesis of several neurodegenerative diseases including sporadic and familial amyotrophic lateral sclerosis (ALS and FALS), Alzheimer's disease (AD), Parkinson's disease (PD), Huntington's disease (HD) and related polyglutamine (polyQ) expansion diseases as well as transmissible spongiform encephalopathy (TSE) diseases.[1–5] Heat shock proteins (HSPs) are molecular chaperones whose expressions are induced as part of the cellular stress response. HSPs recognize and either repair or destroy misfolded proteins.

Increased expression of many HSPs is regulated at least in part by the activation of heat shock transcription factor-1 (HSF1).[6–9] Up-regulation of heat shock proteins (HSPs) via small molecules has shown great therapeutic promise in a number of disease areas where the probable common cause is the accumulation of misfolded proteins.[10–12] For example, Arimoclomol is now in phase II/III clinical trial in ALS patients,[11] and Celastrol is in clinical trial for treating rheumatoid arthritis.[12] Several therapeutically active small molecules that increase cellular HSP levels have been reported (e.g., celastrol, radicicol, galdanamycin, 17-AAG). These compounds seem to mediate their effect on HSPs by indirect activation of HSF1.[13] Other compounds, exemplified by bimoclomol arimoclomol, and iroxanadine do not activate HSF1 or induce HSP expression in normal unstressed cells, but only amplify the already activated chaperone response in stressed or diseased cells that accumulate misfolded proteins.[10] Such a unique molecular mechanism that specifically targets stressed cells potentially offers greater safety than compounds that induce the chaperone response in all cells indiscriminately.[10] Our interest is to discover more potent small molecule chaperone amplifiers to effectively treat neurodegenerative diseases and other diseases of protein misfolding.

Previous investigation revealed that the transcriptional activity of HSF1 in cultured cells correlated well with the formation of intranuclear HSF1 granules.[14,15] Hence we developed a quantitative high-throughput assay for HSF1 transcriptional activity using

* Corresponding author. Tel. +1 858 273 2501x221; fax: +1 858 273 2697.
E-mail address: yuefen.zhou@gmail.com (Y. Zhou).

0960-894X/$ - see front matter © 2009 Published by Elsevier Ltd.
doi:10.1016/j.bmcl.2009.03.011

Table 1
The percentage of HSF1 granule formation (average) with or without heat shock stress

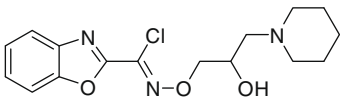

1

% of granule formation (standard deviation)	DMSO	Compound **1**
No heat shock stress (37 °C)	5.6 (±0.7)	6.7 (±0.91)
Heat shock stress (41 °C)	7.3 (±1.2)	58.0 (±4.0)

high content image-based HSF1 granule formation in heat-shocked HeLa cells in order to screen for potential amplifiers of HSF1.[16] We began our screening efforts with an in-house directed library containing compounds structurally similar to arimoclomol, bimoclomol, and iroxanadine. We discovered that chloro-oxime **1** showed potent HSF1 amplification activity (Table 1). Treatment with **1** resulted in a significant increase in the percentage of cells with active HSF1 granules following mild heat shock compared to cells treated with **1** without heat shock (58% vs 7.3%, respectively). However, there is no noticeable change in granule formation when cells were treated with **1** at non-stress conditions (6.7% vs 5.6%), suggesting that **1** by itself is not a stressor. Thus, **1** is a bona fide amplifier of HSF1 activity, not a de novo activator of HSF1. In addition, **1** also increased HSP70 expression under identical heat shock condition (41 °C with 2 h recovery time) with maximum percentage activation of 51% (EC_{50} = 32.9 μM) indicating that compound **1** is a HSF1/HSP70 co-inducer.[17] We focused on lead optimization of this chemical series aiming to improve activity for chaperone amplification that would provide cytoprotection in neurodegenerative disease cell models for potential use as targeted chaperone therapies.

The synthesis of the chloro-oxime derivatives was fairly straightforward and there are a number of synthetic methods (**Methods A** and **B**, Schemes 1 and 2)[18] available to prepare the compounds shown in Tables 2–4.

Oximes **2** were synthesized by the reaction of commercially available aldehydes with hydroxylamine under heating conditions in >90% yield. Alternatively oximes **2** could be provided by a one step synthesis directly from *ortho*-hydroxyanilines **3** by treatment with 2,2,2-trichloro-1-ethoxyethanol in good yields.[19] Oximes **2** were then treated with thionyl chloride to form nitriles **4** which were then converted to hydroxyimidamides **5** by treating with hydroxylamine in good yield. Compounds **5** were then converted to the key intermediates **8** in moderate yields by treating with quaternary azetidinium salts **7** in the presence of a base under heating. Azetidinium salts **7** were synthesized by reacting epichlorohydrin with secondary amines **6** under heating in moderate yields.[20] The key intermediates **8** were then treated with $NaNO_2$ and HCl to provide the desired chloro-oxime derivatives **9** in low to good yields. Alternatively in **Method B** (Scheme 2), hydroxyimidamides **5** were directly treated with epichlorohydrin to form compounds **10** in moderate to good yields, which were then treated with either amines **6** or methyl sulfonamide to form key intermediates **8** or **11** in ⩾80% yields. Intermediates **8** and **11** were then converted to the desired products **9** and **12** respectively in the same way as that described in **Method A**. Methods **A** and **B** diverge at compounds **5**. For most substrates, both methods worked equally well. However, in some cases reactions of amino-oximes **5** with **7** in **Method A** gave very low yields while **Method B** resulted in fairly good yields. On the other hand, **Method A** is more convergent.

Our lead optimization focused on the modification of the left side (R^1), right side (R^2 and R^3) of the molecules **9** and the replacement of the Cl moiety in the chloro-oxime core to study the structure and activity relationship (SAR). We used the high content image-based HSF1 granule formation in HeLa cells to measure the HSF1 activation activity.[21] Additionally, we developed the MG-132 cell stress model in SK-N-SH neuroblastoma cells to systematically measure the cytoprotection of the analogs in this series.[22] MG-132 is a potent and selective 26S proteasome inhibi-

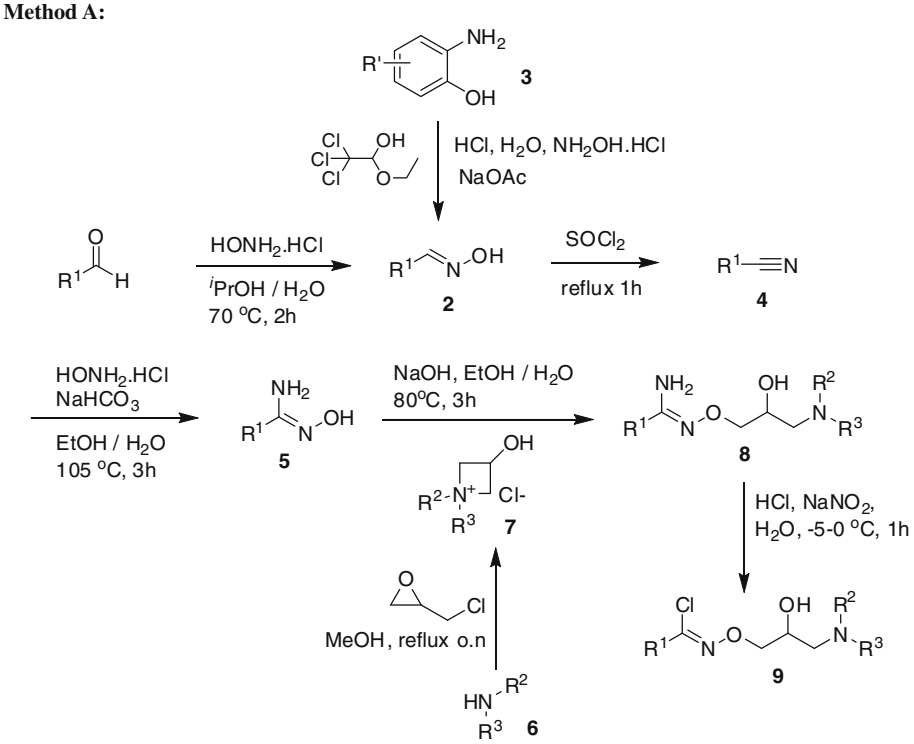

Scheme 1. Synthetic method A for chloro-oxime derivative preparation.

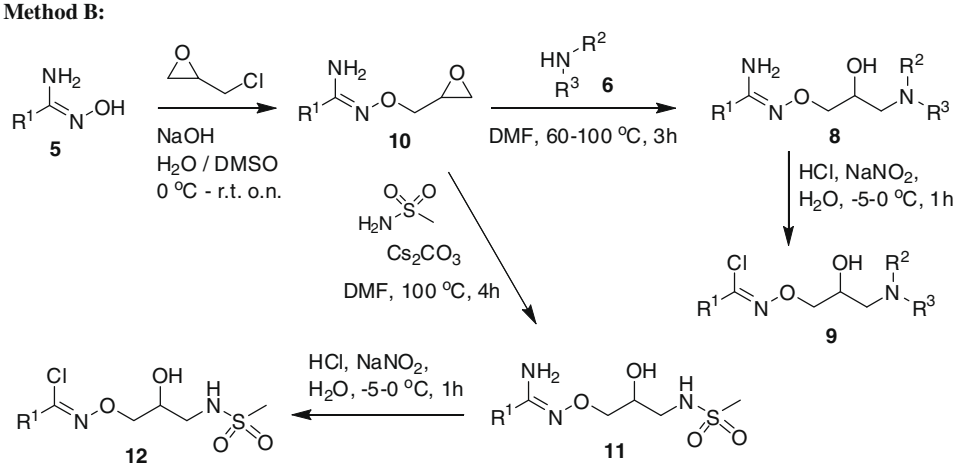

Scheme 2. Synthetic method B for chloro-oxime derivative preparation.

tor that can cause protein misfolding and apoptosis because it inhibits the degradation of ubiquitin-conjugated proteins,[23] In addition, MTS assays in both HeLa and SK-N-SH cells were run to determine the CC_{50} (cytotoxic concentration at 50% of inhibition) values to evaluate the in vitro therapeutic index ($TI = CC_{50}/EC_{50}$).[24] The results of the R^4 (=–NR^2R^3) SAR on the right side of the molecule are summarized in Table 2.

The initial hit (**1**) of the HSF1 amplifier also showed significant cytoprotection in the MG-132 stress assay (Fig. 1).

As shown in Figure 1, when the DMSO control was treated with MG-132, about 30% of cells survived compared with that without MG-132 treatment. However, cell survival (rescue) increased three folds in cells treated with compound **1** compared with MG-132 alone, indicating that the cells were almost fully rescued from MG-132 toxicity.

On the other hand, there was almost no separation between EC_{50} value measured by HSF1 or MG-132 assays and cell toxicity in HeLa or SK-N-SH cells measured by MTS assays for this compound (**1**) (Table 2). Replacing the benzoxazole ring with a benzothiazole moiety (**13**, X = S) retained both the HSF1 activity and cytoprotection from MG-132. Reducing the ring size of R^4 completely diminished the cytoprotection from MG-132 stress although it had weak HSF1 activity (**14**). Interestingly, replacement of piperidine with morpholine moiety of R^4 resulted in a complete loss of HSF1 activity and significant reduction of cytoprotection in MG-132 assay (**15**). Addition of F-atoms on the piperidine ring also reduced the HSF1 activity but restored much of the cytoprotection with reduced cell toxicity in both HeLa and SK-N-SH cells (**16**–**18**). However, addition of electron donating groups on the piperidine ring led to slight improvement in HSF1 activity and cytoprotection from MG-132 stress with improved therapeutic index (**19**–**20**).

When R^4 were acyclic amines, many of them (**21**–**22**, **24**–**26**, **28**–**30**) resulted in some improvement in both HSF1 activity and cytoprotection from MG-132 toxicity compared with the piperidine (**1**). A few of them had single digit μM EC_{50} in the MG-132 assay. However, branching adjacent to the N-atom (**27**) of the tertiary amine moiety (R^4) or longer alkyl groups (**23**) led to decreased HSF1 activity or cytoprotection from MG-132 stress. Furthermore, replacing the terminal methyl group of **28** with a hydroxyl group was well tolerated (**31**). The addition of an F-atom at the terminal tertiary amine group of **28** or replacement of the terminal *n*-propyl group of **28** with cyclopropyl methylene moiety retained HSF1 activity and cytoprotection (**32**–**33**). Other replacements of the terminal tertiary amines including secondary amine, methyl sulfonamide, amide and reversed amide resulted in much weaker or complete loss of HSF1 activity and weaker cytoprotection (**34**–**37**). Overall the right side of the molecule (R^4) had an impact on the HSF1 activity as well as cytoprotection from MG-132 stress.

Next, the R^1 SAR on the left side of the molecule was also studied and the results are summarized in Table 3.

As shown in Table 3, all the substituents on the benzoxazole ring at various positions (4–7), electron withdrawing or donating, resulted in similar or slightly improved HSF1 activity (**38**–**47**) than the non-substituted benzoxazole (**1**). However, the majority of them had improved cytoprotection effect from MG-132 stress with EC_{50} of <10 μM. More importantly, they all showed better therapeutic index comparing with the initial hit (**1**). In addition, (4,5)-naphathyl benzoxazole led to a more potent HSF1 activator (**48**) with significant improvement in cytoprotection from MG-132 stress than the initial hit (**1**). However, its cell toxicity increased. Interestingly, removing the N-atom in the benzoxazole or benzothiazole ring (**49**–**50**) totally diminished the HSF1 activity and cytoprotection effect suggesting that the benzoxazole ring of R^1 is important to the HSF1 activity and cytoprotection from MG-132 stress.

In addition to SAR of the left (R^1) and right sides (R^4) of the molecule, the effect of the middle part of the molecule (Y) on the HSF1 activity and cytoprotection from MG-132 stress was also evaluated (Table 4).

As shown in Table 4, replacement of the Cl atom in the Cl-oxime core with H, CH_3, OCH_3, CF_3 or F moieties (**51**–**55**) completely diminished HSF1 activity and MG-132 cytoprotection although reduced cell toxicity was observed. The amide analog also had no HSF1 activity or MG-132 cytoprotection (**56**). In addition, removing the hydroxyl group of initial hit **1** caused complete loss of HSF1 activity and significant reduction of the MG-132 cytoprotection (**57**). These results suggest that both the Cl moiety in the Cl-oxime core and the hydroxyl group are essential to the HSF1 activity and the MG-132 cytoprotection effect.

It is worth noting that all the compounds tested in this series showed no activity in the HSF1 granule assay in the absence of the heat shock stress (data not shown). Therefore, this class of small molecule chaperone inducers acts like 'smart drugs' by a selective interaction with only those cells in stress, and may provide therapeutic advantages.

In order to evaluate whether this class of compounds has more general and broad cytoprotection effect, some of the compounds in this series were also tested in the tunicamycin-induced endoplasmic reticulum (ER) stress assay.[25] Tunicamycin blocks the maturation of proteins that require glycosylation, resulting in protein

Table 2
SAR of R^4 in HSF1 granule and MG-132 assays

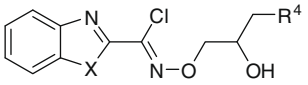

Compound[a]	X	R^4	EC_{50} (HSF1, μM)[b]	EC_{50} (MG-132, μM)[c]	CC_{50} (Hela, μM)[d]	CC_{50} (SK, μM)[d]
1	O	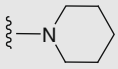	41.7	15.7	41.7	26
13	S	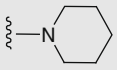	52.6	13.5	49.1	26.5
14	S		62.8	No activity	60.1	31.1
15	O	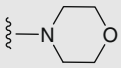	No activity	61.7	>80	>80
16	O	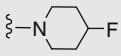	63% @ 80	18.8	35% @ 80	52.6
17	O	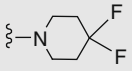	49% @ 80	26.4	>80	>80
18	O	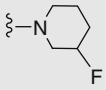	52.6	20	52.7	49.8
19	O		17.4	9.3	55.3	34
20	O		32.4	11.1	78.9	36.2
21	O	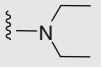	27.1	10.2	NT[e]	NT[e]
22	O	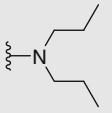	23.9	10.2	66% @ 80	46.4
23	O	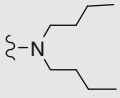	20.9	22.3	>80	41
24	O	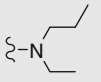	23	12.4	40.7	42.1
25	O	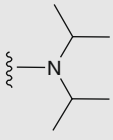	25.5	14.7	45	30.8
26	O	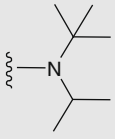	16.6	9.9	45.7	40.3

(*continued on next page*)

Table 2 (*continued*)

Compound[a]	X	R^4	EC_{50} (HSF1, μM)[b]	EC_{50} (MG-132, μM)[c]	CC_{50} (Hela, μM)[d]	CC_{50} (SK, μM)[d]
27	O		62% @ 80	20.9	38% @ 80	54.2
28	O	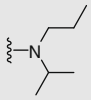	24.1	8.9	57.6	50.4
29 (*R*)[f]	O	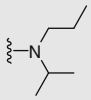	28.6	7.1	67.8	25
30 (*S*)[f]	O	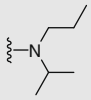	31.9	7.8	59.9	31.1
31	O	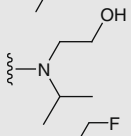	28.7	8.2	50.2	30.6
32	O	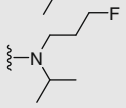	22.8	10.1	33.8	46
33	O	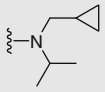	12.4	6.3	24.4	32.7
34	O	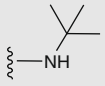	25% @ 80	No activity	55.4	24.7
35	O	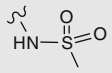	No activity	39.3	48.5	>80
36	O		No activity	41.9	>80	>80
37	O	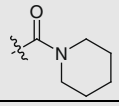	28% @ 80	43.6	46.9	59.6

[a] The desired mass was found for each compound in LC–MS analysis. ^{1}H NMR spectra are consistent with their structures. All the compounds showed no activity in HSF1 granule assay without heat shock stress.
[b] See Ref. 21 (for HSF1 granule assay condition).
[c] See Ref. 22 (for MG-132 stress assay condition).
[d] See Ref. 24 (for MTS assay condition).
[e] NT=not tested.
[f] >95% ee based on the chiral HPLC analysis.

retention and stress induction in the endoplasmic reticulum. In this assay, the differentiated PC12 cells were treated with tunicamycin in the presence of selected compounds at 37 °C for 43 h. Cell viability was measured with ATPlite and percentage of increased ATP was calculated by comparing with the DMSO control with tunicamycin treatment alone. For the compounds tested (**1**, **25** and **28**), excellent cytoprotection from ER stress was observed (>200%, >150% and ~300%, respectively) as shown in Figure 2.

Next, in order to further evaluate the potential applications of this series of chloro-oxime derivatives, the cytoprotection effect of selected compounds in biologically relevant cell models was also investigated. The polyQ-Htt model that expresses the misfolded Huntingtin protein is a cell-based model system for Huntington's disease. In this assay,[26] stably transfected and doxycycline (DOX) inducible polyQ 145-Htt cells were used. When protein expression was induced by DOX, Q145 expressing cells showed about 40% cell viability compared with non-induced cells measured by MTS. In the presence of either compounds **1** or **25**, significant cell protection was observed resulting in 77% and 58% increase in cell number, respectively, as compared with the DMSO control with DOX treatment indicating that the cells were fully rescued from polyQ toxicity (Fig. 3). This result encourages us to evaluate more compounds of this class in the polyQ cell model in the future.

In order to evaluate the possibility that the increase in cell viability observed above may be caused by stimulation of cell proliferation rather than inhibition of cell death by the compounds tested, additional experiments were run using Click-iT cell proliferation assay (data not shown) with selected compounds. We found

Table 3
SAR of R^1 in HSF1 granule and MG-132 assays

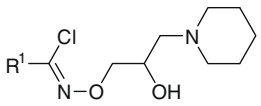

Compound	R^1	EC_{50} (HSF1, μM)	EC_{50} (MG-132, μM)	CC_{50} (Hela, μM)	CC_{50} (SK, μM)
1	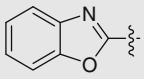	41.7	15.7	41.7	26
38	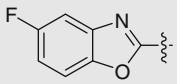	51.3	12	>80	62.4
39	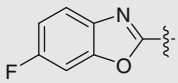	29.4	11	>80	37.3
40	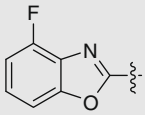	20.2	6.9	40.2	20.3
41	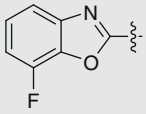	18.5	3.8	19.3	16.9
42	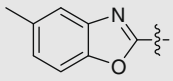	41.6	9.5	65% @ 80	34.6
43	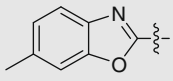	31	6.1	18.8	28
44	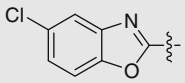	20.9	6.3	31.4	23.2
45	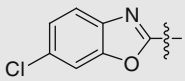	22.9	9	44.2	20
46	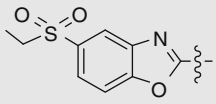	42.9	5.9	41.4	44.2
47	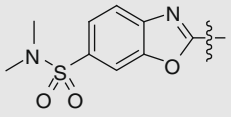	41.6	7.9	45.1	42.4
48	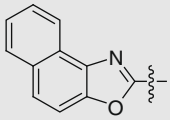	12.1	5.2	18.9	17.4
49	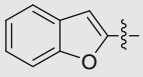	No activity	No activity	>80	>80
50	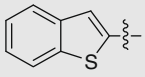	No activity	No activity	>80	67.7

Table 4
SAR of Y in HSF1 granule and MG-132 assays

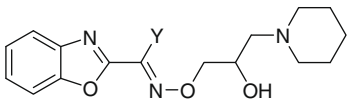

Compound	Product or Y	EC_{50} (HSF1, μM)	EC_{50} (MG-132, μM)	CC_{50} (Hela, μM)	CC_{50} (SK, μM)
1	Cl	41.7	15.7	41.7	26
51	H	No activity	No activity	>80	>80
52	CH_3	No activity	No activity	>80	>80
53	OCH_3	No activity	No activity	>80	>80
54	CF_3	No activity	No activity	>80	>80
55	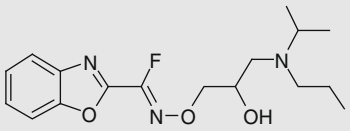	No activity	No activity	>80	>80
56	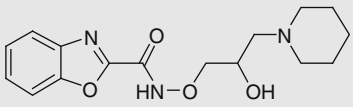	No activity	No activity	>80	>80
57	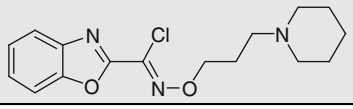	No activity	58.7	>80	>80

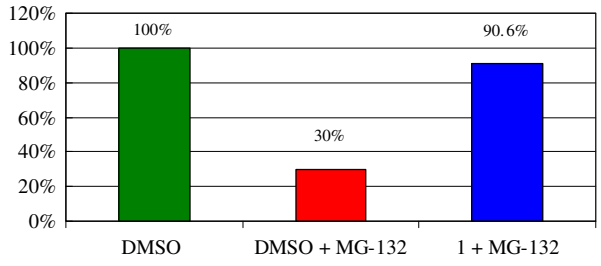

Figure 1. The percentage of cell numbers of compound **1** with MG-132 treatment compared with the DMSO control.

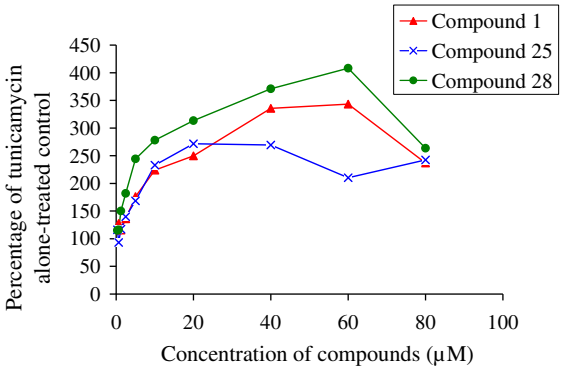

Figure 2. Effect of compounds on the viability of differentiated PC12 cells treated with tunicamycin for 43 h as compared with the DMSO control treated with tunicamycin (normalized to 100%).

that neither compound **1** nor **28** caused any cell proliferation up to 20 μM tested in HeLa cells while in SK-N-SH cells both above compounds significantly decreased cell proliferation in the compound concentration range tested (0–20 μM). These results ruled out the possibility of compound-induced proliferation effect in these assays, and the cytoprotection observed is likely via the molecular chaperone amplification mechanism.

In summary, we synthesized a number of chloro-oxime derivatives as novel small molecule chaperone amplifiers. Our SAR studies revealed that the Cl moiety at the chloro-oxime core played the essential role in the HSF1 activation activity and cytoprotection from MG-132 stress. In addition, both left (R^1) and right sides (R^4) of the molecules had effects on activity and cell toxicity. Many compounds under study showed excellent cytoprotection in the MG-132 stress cell model with single digit micro molar potency. Among them, a few compounds further showed great cytoprotection in ER stress and polyQ-Htt cell models, suggesting that they may have broad utility in neurodegenerative diseases. As the pol-

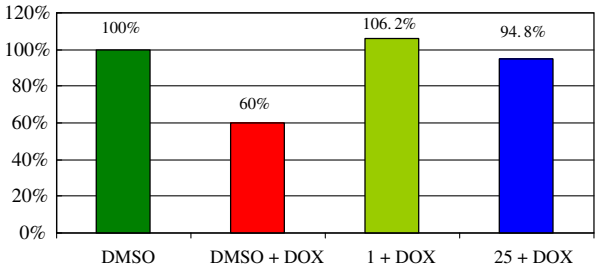

Figure 3. The percentage of polyQ 145-Htt cell numbers of compound **1** and **25** induced by DOX compared with the DMSO control.

yQ-Htt cell stress model is directly relevant to the Huntington's disease (HD), this class of compounds potentially could be used as a new therapeutic approach in treating polyglutamine expansion neurodegenerative diseases such as Huntington's disease.

References and notes

1. Leigh, P. N.; Whitwell, H.; Garofalo, O.; Buller, J.; Swash, M.; Martin, J. E.; Gallo, J.-M.; Weller, R. O.; Anderton, B. H. *Brain* **1991**, *114*, 775.
2. Agorogiannis, E. I.; Agorogiannis, G. I.; Papadimitriou, A.; Hadjigeorgiou, G. M. *Neuropathol. Appl. Neurobiol.* **2004**, *30*, 215.
3. Muchowski, P. J.; Wacker, J. L. *Nat. Rev. Neurosci.* **2005**, *6*, 11–22.
4. Walsh, D. M.; Selkoe, D. J. *Protein Pept. Lett.* **2004**, *11*, 213.
5. Caughey, B.; Lansbury, P. T. *Annu. Rev. Neurosci.* **2003**, *26*, 267.
6. Shi, Y.; Moser, D. D.; Morimoto, R. I. *Genes Dev.* **1998**, *12*, 654.
7. Christians, E. S.; Yan, L. J.; Benjamin, I. J. *Crit. Care Med.* **2002**, *30*, S43.
8. Voellmy, R. *Cell Stress Chaperones* **2004**, *9*, 122.
9. Pirkkala, L.; Nykänen, P.; Sistonen, L. *FASEB J.* **2001**, 1118.
10. Sõti, C.; Nagy, E.; Giricz, Z.; Vígh, L.; Csermely, P.; Ferdinandy, P. *Br. J. Pharmacol.* **2005**, *146*, 769.
11. Boggs, J. *BioWorld Today* **2009**, *20*, 1.
12. Corson, T. W.; Crews, C. M. *Cell* **2007**, *130*, 769.
13. Westerheide, S. D.; Morimoto, R. I. *J. Biol. Chem.* **2005**, *280*, 33097.
14. Cotto, J.; Fox, S.; Morimoto, R. I. *J. Cell Sci.* **1997**, *110*, 2925.
15. Nonaka, T.; Akimoto, T.; Mitsuhashi, N.; Tamaki, Y.; Nakano, T. *Cancer Lett.* **2003**, *202*, 89.
16. Au, Q.; Kanchanastit, P.; Barber, J. R.; Ng, S. C.; Zhang, B. *J. Biomol. Screen* **2008**, *13*, 953.
17. *HSP70 granule assay condition*: The assay was performed according to the previous publication (Ref. 16) which was very similar to the HSF1 granule assay as described in Ref. 21. Briefly, immunocytochemical staining for HSP70 was performed 2 h after heat shock at 41 °C. Automatic image acquisition was performed using an INcell 1000 analyzer and analysis was carried out using Multi Target Analysis (MTA) module from Workstation 3.6 for quantification of the HSP70 granule count and total granule area.
18. Nagy, P. L.; Balvázs, B.; Boross, M.; Szilbereky, J.; Zsila, G.; Ăbrahám L.; Blaskó, G.; Gachályi, B.; Almási, A.; Német, G. U.S. Patent 5,147,879, 1992.
19. Huang, F.-C. U.S. Patent 4,368,201, 1983.
20. a Dressman, B. A.; Godfrey, A. G. WO 00/38685, 2000.; (b) Gaertner, V. R. *J. Org. Chem.* **1968**, *33*, 523; (c) Gaertner, V. R. *Tetrahedron Lett.* **1967**, 343.
21. *HSF1 granule assay condition*: The assay was performed according to the previous publication (Ref. 16). Briefly, *HeLa* cells were pretreated with compounds 1 h before heat shock at 41 °C for 2 h with no recovery time. As a control, *HeLa* cells were pretreated with compounds at 37 °C for 3 h in order to eliminate compounds that induce heat shock response in the non-stress cells. The overall dilution of compound was 200-fold, with a concentration ranging from 0.3 μM to 80 μM. Immunocytochemical staining for HSF1 in *HeLa* cells was performed following the previous publication with some modifications (Ref.: Zhang, B.; Gu, X.; Uppalapati, U; Ashwell, M. A.; Leggett, D. S.; Li, C. J. *J. Biomol. Screen* **2008**, *13*, 538). Image acquisition was performed using an INcell 1000 analyzer (GE Healthcare, Piscataway, NJ) with a 10× object. Image analysis was carried out using Multi Target Analysis module from Workstation 3.6. Algorithms for the HSF1 total granule counts, granule area and nuclear intensity coefficient of variation (CV) were established according to assay conditions and manufacture instructions. EC_{50} values and curve fitting were calculated using PRISM 4.0 (GRAPHPAD Software, San Diego, CA) with nonlinear regression analysis. The maximum percentage of cells that have positive granule formation >20% is considered active. The compounds were tested in the concentration range of 0.3–80 μM with twofold dilution. EC_{50} value is the concentration at which 50% of cells have positive granule formation. The average standard deviation for the data in Tables 2 and 3 generated from this assay was 34% for multiple testing of same compounds in different runs.
22. *MG-132 stress assay condition*: SK-N-SH cells at 12,500 cells/well were pretreated with compounds one hour before addition of MG-132 at a final concentration of 5 μM for 24 h. Compound **1**, an in house compound serves as a positive control and DMSO as a negative control. Cell viability was measured with ATPlite-1step (Perkin Elmer) according to manufacturer's protocol. Percentage of increased ATP was calculated using the following formula (RLU, relative luminescent unit): Increased ATP% = $(RLU_{compound} - RLU_{DMSO})/RLU_{DMSO} \times 100\%$. EC_{50} values and curve fitting were calculated using PRISM 4.0 (GRAPHPAD Software, San Diego, CA) with nonlinear regression analysis. EC_{50} value is the concentration at which the cell numbers increase 50% by comparing with MG-132 treatment alone without compound. The compounds were tested in the concentration range of 0.3–80 μM with twofold dilution and the maximum percentage of the cytoprotection >60% is considered active. The average standard deviation for the data in Tables 2 and 3 generated from this assay was 26% for multiple testing of same compounds in different runs.
23. Lee, D. H.; Goldberg, A. L. *Trends Cell Biol.* **1998**, *8*, 397.
24. *MTS assay condition*: *HeLa* (4000 cells/well) and SK-N-SH (14,000 cells/well) were seeded in DMEM containing 10% FBS for 18 h before experiment. Compounds or DMSO control were added to the culture at 1–200 dilutions with a final concentration ranging from 0.3 μM and 80 μM. MTS assay was performed according to a published protocol (Ref.: Zhang, B.; Gu, X. Uppalapati, U.; Ashwell, M. A.: Leggett, D. S.; Li, C. J., *J Biomol. Screen* **2008**, *13*, 538). Percentage of inhibition was determined using the following formula:$(MTS_{DMSO} - MTS_{compound})/MTS_{DMSO} \times 100\%$. CC_{50} values and curve fitting were calculated using PRISM 4.0 (GRAPHPAD Software, San Diego, CA) with nonlinear regression analysis. The average standard deviation for the data in Tables 2 and 3 generated from MTS_Hela and MTS_SK assays were 34% and 14%, respectively, for multiple testing of same compounds in different runs.
25. *Tunicamycin-induced endoplasmic reticulum (ER) stress assay condition*: PC12 cells were plated at a density of 5000 cells/well in 96-well plates. NGF was added to a final concentration of 50 ng/ml to induce differentiation for 5–7 days with neurite outgrowth observed. The differentiated PC12 cells were treated with compound (1:20 dilution) and Tunicamycin (final concentration at 750 ng/mL) for 43 h at 37 °C. Cell viability was measured with ATPlite (PerkinElmer) according to the manufacture's instruction. Percentage of increased ATP was calculated using the following formula (RLU, relative luminescent unit): Increased ATP% = $(RLU_{compound} - RLU_{DMSO})/RLU_{DMSO} \times 100\%$. EC_{50} values and curve fitting were calculated using PRISM 4.0 (GRAPHPAD Software, San Diego, CA) with nonlinear regression analysis.
26. *PolyQ-Htt induction model condition*: The stable polyQ 145-Htt cells (5000 cells per well) were treated with doxycycline (10 μg/mL) for 6 days in the presence or absence of test compounds (0.3–60 μM). Cell viability was then measured with MTS assay. The cytoprotection of compounds in polyQ-Htt induction model is defined as following: $(MTS_{compound} - MTS_{polyQ\ alone})/MTS_{polyQ\ alone} \times 100$ (%).